DOI: 10.1007/s11430-006-2003-z

Thermal regimes and degradation modes of permafrost along the Qinghai-Tibet Highway

JIN Huijun, ZHAO Lin, WANG Shaoling & JIN Rui

State Key Laboratory of Frozen Soils Engineering and Cryosphere Station of the Qinghai-Tibet Plateau, Cold and Arid Regions Environmental and Engineering Research Institute, Chinese Academy of Sciences, Lanzhou 730000 China

Correspondence should be addressed to Jin Huijun (email: hjjin@lzb.ac.cn)

Received September 20, 2005; accepted April 10, 2006

Abstract Permafrost on the Qinghai-Tibet Plateau (QTP) is widespread, thin, and thermally unstable. Under a warming climate during the past few decades, it has been degrading extensively with generally rising ground temperatures, the deepening of the maximum summer thaw, and with lessening of the winter frost penetration. The permafrost has degraded downward, upward and laterally. Permafrost has thinned or, in some areas, has totally disappeared. The modes of permafrost degradation have great significance in geocryology, in cold regions engineering and in cold regions environmental management. Permafrost in the interior of the QTP is well represented along the Qinghai-Tibet Highway (QTH), which crosses the Plateau through north to south and traverses 560 km of permafrost-impacted ground. Horizontally, the degradation of permafrost occurs more visibly in the sporadic permafrost zone in the vicinity of the lower limit of permafrost (LLP), along the margins of taliks, and around permafrost islands. Downward degradation develops when the maximum depth of seasonal thaw exceeds the maximum depth of seasonal frost, and it generally results in the formation of a layered talik disconnecting the permafrost from the seasonal frost layer. The downward degradation is divided into four stages: 1) initial degradation, 2) accelerated degradation, 3) layered talik and 4) finally the conversion of permafrost to seasonally frozen ground (SFG). The upward degradation occurs when the geothermal gradient in permafrost drops to less than the geothermal gradients in the underlying thawed soil layers. Three types of permafrost temperature curves (stable, degrading, and phase-changing transitory permafrost) illustrate these modes. Although strong differentiations in local conditions and permafrost types exist, the various combinations of the three degradation modes will ultimately transform permafrost into SFG. Along the QTH, the downward degradation has been proceeding at annual rates of 6 to 25 cm, upward degradation at 12 to 30 cm, and lateral degradation in the sporadic permafrost zone at 62 to 94 cm during the last quarter century. These rates exceed the 4 cm per year for the past 20 years reported for the discontinuous permafrost zone in subarctic Alaska, the 3 to 7 cm per year reported in Mongolia, and that of the thaw-stable permafrost in subarctic Yakutia and Arctic Alaska.

Keywords: QTP, QTH, permafrost, ground temperatures, degradation modes, geothermal gradients.

The Qinghai-Tibet Plateau (QTP) has the largest expanse, about 1.3×10^6 km^2, of elevational permafrost on earth. High elevation, active tectonics, complex Quaternary deposits, cold and relatively dry climate, high solar radiation and heat budget control the formation and evolution of permafrost. The main body of existing permafrost was formed during the Last Glaciation Maximum (LGM) in the late Pleistocene[1−3]. Permafrost developed time and again after the periods of degradation under climatic fluctuations with a general warming trend since the post-glacial periods[2]. The distribution of permafrost was controlled by elevational zonation with strong influences of latitudinal and longitudinal (aridity) zonation[4]. On the basis of 3-directional zonation, other local geological and geographical factors also played roles of varied importance. Compared with the subarctic continental regions, the climate on the QTP is characterized by small annual ranges of air temperatures (mild winters and cool summers, and without clear division of four seasons), resulting in shallow depths of annual zero amplitude in ground temperatures[1)] and widespread distribution of thin and unstable permafrost[3,5,6]. Under a persistent trend of warming climate during the past several decades, permafrost has been in general degradation[7−9]. In addition, increasingly frequent and intensive engineering activities have greatly impacted the stability of permafrost[10,11], inevitably resulting in a variety of environmental distresses[5,12,13], particularly on the alpine ecosystems, engineering construction and the regional water and land resources[14].

Reasonable understanding of the modes and processes of permafrost degradation under the combined influences of climate warming and human activities is very important. The reliability and long-term stability of engineering foundations, cold regions environmental management, hazards mitigation, and utilization and conservation of land and water resources are dependent on these understandings. Studies on the stability of the cryosphere and climatic systems, reconstruction of paleo-climate and paleo-environment, and the forecast of future trends of climatic are needed for understanding the permafrost changes. However, the observations and modeling on the degradation modes of permafrost have been very limited to date[15,16]. Most of the studies on the degradation of permafrost focus on how much permafrost has disappeared, rather than how it has been lost. Therefore, it is rather difficult to evaluate the impacts of degrading permafrost and to provide scientific bases for engineering design, construction, environmental management and policy making. In the continuous permafrost zone, permafrost mainly degrades through slow upward thawing induced by thermal conduction. On the marginal areas of the discontinuous permafrost zone, climatic warming of several degrees can have major impacts on the thermal regimes of permafrost on a timescale of years or tens of years. Warm (>−1℃), discontinuous permafrost has been degrading rapidly, but little has been understood concerning the mechanisms and modes of its degradation due to the paucity of data on the thawing rates at the permafrost table and at its base, the processes of talik development, the timescales involved in thawing, and lateral geothermal fluxes.

During the past several decades, thousands of boreholes have been drilled in permafrost for engineering design and construction of the QTH, the Qinghai-Tibet Railway, the Golmud to Lhasa Oil Products Pipeline, and scientific research programs[7,14]. Data on ground temperatures from 60 boreholes with observation periods longer than three years and observation depths greater than 20 m were chosen for comparison and contrasting in this paper. In the 1960s to 1970s, chains of Assmann thermometers with an accuracy of ±0.1℃ were used in manually reading ground temperatures in boreholes on a weekly basis. In the 1980s, thermistor cables were more often used in combined manual and automatic reading of ground temperatures in boreholes. During the 1990s and early 2000s, thermistor cables and data loggers with accuracies of better than ±0.1℃ have been widely used. The exact latitudes, longitudes and elevations of boreholes were generally obtained either from 1∶100,000 topography maps, or measured by the global positioning systems (GPS), levels or theodolites with accuracies of 1″

1) For ease of discussion, the mean annual ground temperature (MAGT) at the depth of zero annual amplitude of ground temperatures is differentiated from the average annual soil temperature (AAST) at any depth in a soil temperature profile.

(or less) in latitudes and longitudes and 1 m (or less) in elevation. The data from the 60 boreholes are categorized, and representative ground temperature curves are plotted for analyses.

1 Typical permafrost temperatures curves

Ground temperatures are very important indicators of thermal regimes in permafrost. Typical ground temperature curves at depths greater than 15—30 m can reveal the formation and evolution history of permafrost at various timescales, and can indicate present thermal regimes and trends of probable changes. Under a general degradation trend of permafrost, there are three geothermal flow conditions in permafrost layers. The three basic types of permafrost temperature curves were divided accordingly based on ground temperature data measured from the 60 boreholes. Permafrost degraded when the overlying soils were warmer than the underlying soils within the depth to zero annual amplitude of ground temperatures, i.e., permafrost absorbed heat, resulting in a "degrading permafrost temperature profile"[17]. Otherwise, permafrost is stabilized by releasing heat, resulting in "stable permafrost temperature curves". However, in some boreholes, soil temperatures in the upper and lower parts were almost the same, or the soils at the upper part are absorbing heat and those at the lower part were cooling, and the thermal gradient was close to zero, with significant lateral heat transfer. In some sections, permafrost has been degrading substantially during the past several decades, with only 1 to 2 m thickness of permafrost remaining. This type is called a "phase-changing transitory permafrost temperature curve". Degrading and phase-changing transitory permafrost temperature curves accounted for 76.7% in the total number of boreholes studied, while the stable type for only 23.3%, indicating a conspicuous regional trend of permafrost degradation (Table 1).

Table 1 Types of permafrost temperature curves and their percentage in the studied 60 boreholes

Type	Borehole number	Percentage (%)
Degrading	31	51.7
Stable	14	23.3
Phase-changing transitory	15	25.0
Total	60	100.0

The characteristics of each type of permafrost temperature curve are as follows:

1.1 Stable permafrost temperature curves

Stable permafrost temperature profiles were generally observed in alpine areas and in the foothills in the continuous permafrost zone with mean annual ground temperatures (MAGTs) colder than −1.5℃ and thicker permafrost. The average annual soil temperatures (AASTs) in the upper part were generally lower than that in the lower part, with geothermal gradients of 0.03 to 0.05℃ m^{-1} within the depths subject to seasonal fluctuations of ground temperatures. The typical ground temperature curves were observed in the Borehole No. 1 of the Hoh'xil Observation Site, the Borehole at the Kunlun Mountain Pass Ground Temperature Observation Site, and the Borehole at the Meteorological Station in the Fenghuo Mountains (Fig. 1). However, in some boreholes, the AASTs at depths

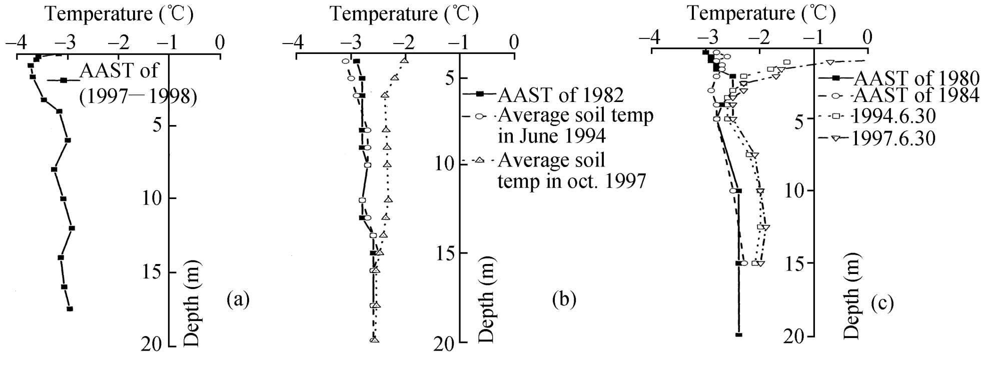

Fig. 1. Typical stable permafrost temperature curves. (a) Borehole No. 1 at the Hoh'xil Observation Site; (b) ground temperature borehole at the Kunlun Mountain Pass; (c) borehole at the Meteorological Site of the Fenghuo Mountains Permafrost Station.

of 0 to 0.4 m are higher than the underlying soil layers as a result of persistent warming during the past few years (Fig. 1(a)).

1.2 Degrading permafrost temperature curves

The degrading permafrost temperature curves were generally observed in valleys and basins on the high plateaus along the margins of the discontinuous permafrost zone and in the island permafrost zones, with MAGTs of –0.5 to −1.5℃. This type of permafrost is generally thin and thermally unstable. The AASTs, between ground surface and the depth of zero annual amplitude of ground temperatures, are higher near the surface, then decline with depths sometimes to even below that of zero change, before increasing with depth due to the positive geothermal gradients. Typical ground temperature curves were observed in the Borehole at the Undisturbed Observation Site at Highway Maintenance Squad (HMS) 66, Borehole K2596, Borehole 113-5, and the borehole at the Northern Outlet of the Jingxiangu Valley (Fig. 2).

1.3 Phase-changing transitory permafrost temperature curves

Phase-changing transitory permafrost temperature curves are mainly encountered on the margins of permafrost islands and around taliks with MAGTs generally higher than –0.5℃. Generally, permafrost in these areas is very thin and unstable; geothermal gradients are generally less than 0.03℃ m^{-1}, sometimes even zero. This type of permafrost temperature curve resembles those of degrading permafrost in the upper part, but with the strong influence of lateral heat fluxes. Under a persistently warming climate, vertical geothermal gradients in permafrost have changed substantially. At a given position, this change can modify stable permafrost to degrading or even the phase-changing transitory type, and ultimately to seasonally frozen ground (SFG). The typical permafrost temperature curves are illustrated by data from the Boreholes at No. 1 and No. 2 Observation Sites at Liangdaohe, Boreholes No. 3 and No. 4 at Xidatan, Borehole 103-II-1, and the four boreholes in the Liangdaohe Basin (Fig. 3).

The permafrost temperature curve at the Liangdaohe No. 1 Observation Site can be divided into three

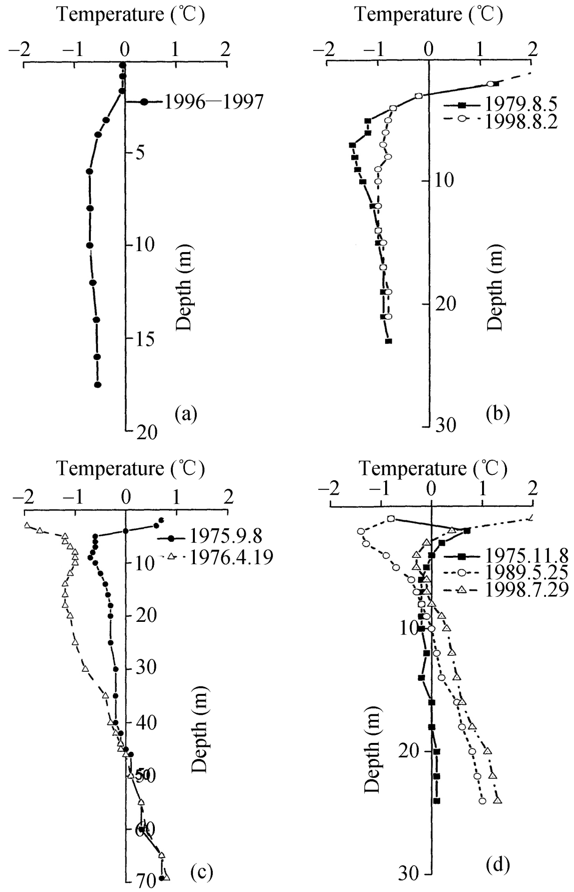

Fig. 2. Typical degrading permafrost temperature curves. (a) Borehole No. 1 at the Undisturbed Site at the HMS 66 on the Cumar River High Plateau; (b) borehole K2596 at the western side of the Qingshui River; (c) borehole 113-5 on the southern foothill of the Taoerjiu Mountains; (d) borehole at the Northern Outlet of the Jingxiangu Valley in the western section of the Xidatan.

sections: the section of permafrost above 4 m in depth fluctuates under the influence of seasonal freeze-thaw processes; the section from 4 to 18 m is affected by the overlying and underlying permafrost with geothermal gradients approximating zero; the section between 18 to 40 m has a slight positive geothermal gradient of about 0.015℃ m^{-1}. This indicates that the upper part of permafrost in the Liangdaohe Basin, formed early in geohistory, has been degrading under a warming climate. As a result, the zero geothermal gradient section between depths of 4 and 18 m has been gradually deepening. In comparison, the geothermal gradient between depths of 15 to 59.8 m is only 0.01℃ m^{-1} in the adjacent Borehole CK7. The observations on 1 July 1995 indicates that the ground temperature at the depth of 59.8 m had risen by 0.1℃, which is attributed

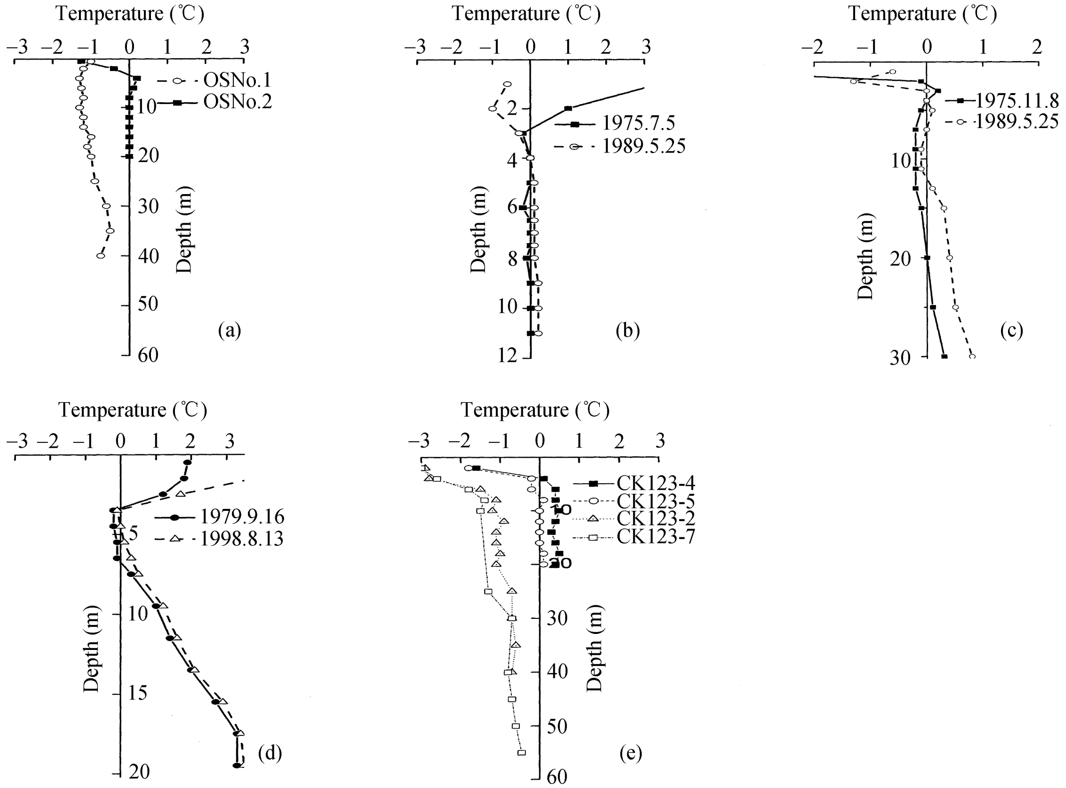

Fig. 3. Typical phase-changing permafrost temperature curves. (a) Boreholes at the Observation Sites No. 1 and No. 2 in Liangdaohe; (b) borehole Xidatan-3; (c) borehole Xidatan-4; (d) borehole 103-II-1 in the Wenquan Valley; (e) boreholes in the Liangdaohe Basin (16 April, 1976).

to the warming during the last few decades.

The three types of permafrost temperature curves are clear manifestations of different stages of permafrost formation, development and degeneration at different spatio-temporal scales; therefore, the division is relative. One type can be transformed to the other at one position under external influences such as climatic change.

2 Modes of permafrost degradation

The direction and intensity of heat flows in permafrost soils change in accordance with shifts in environmental conditions, mainly including air and ground surface temperatures and geothermal flows. If there are only changes in the intensity of heat exchanges, permafrost still can exist or develop. However, when the heat flow reverses in direction, permafrost eventually thaws when MAGTs are persistently no less than the freezing temperatures of soils. Under a warming climate, and subsequent rising ground surface temperatures, heat transfer in soil strata have been changing, resulting in marked changes in geothermal gradients. Permafrost with degrading and phase-changing transitory temperature curves degrades more readily, conspicuously and rapidly[5,7,12,14]. Horizontally, degradation of permafrost occurs first in the vicinity of the northern and southern LLPs, and on the margins of taliks[5,7,9,12]. Vertically, permafrost can degrade downwards, upwards and laterally. Three modes of permafrost degradation exist in almost any area (or depth of soil), with varying degrees of mode combinations. The ultimate results of permafrost degradation are either thinning of permafrost layer(s), or transformation of permafrost to SFG.

2.1 *Downward degradation of permafrost*

The responses of permafrost to changes in air temperatures are determined by initial ground surface temperatures, soil temperatures, thermal properties of soils, water contents, distribution of ground ice, and geothermal flows. Except ground surface temperatures, other factors can be regarded as largely constant in the reasonably long-term. Therefore, seasonal freezing and thawing can be approximated as a single variable function of air temperatures. At a given location, when air temperatures reach a threshold, the maximum seasonal thaw penetration is greater than the maximum seasonal frost penetration, and subsequently the permafrost table drops, disconnecting permafrost from the seasonal frost layer with a layered talik. When the talik thickens year after year, permafrost is eroded downwards[5,7,14]. Observations indicate that in most of the boreholes, there was a conspicuous warming in ground temperatures in the upper part of permafrost between the 1970s and 1980s or 1990s. The AASTs at various depths were calculated in order to study the evolution processes of ground temperature curves in downward degrading permafrost from 12 boreholes with data series longer than 1 to 3 years in the 1990s (Table 2).

According to the changes in ground temperatures near the permafrost table during the past several years, the process of downward degradation of permafrost can be further divided into four stages from permafrost to SFG (Fig. 4).

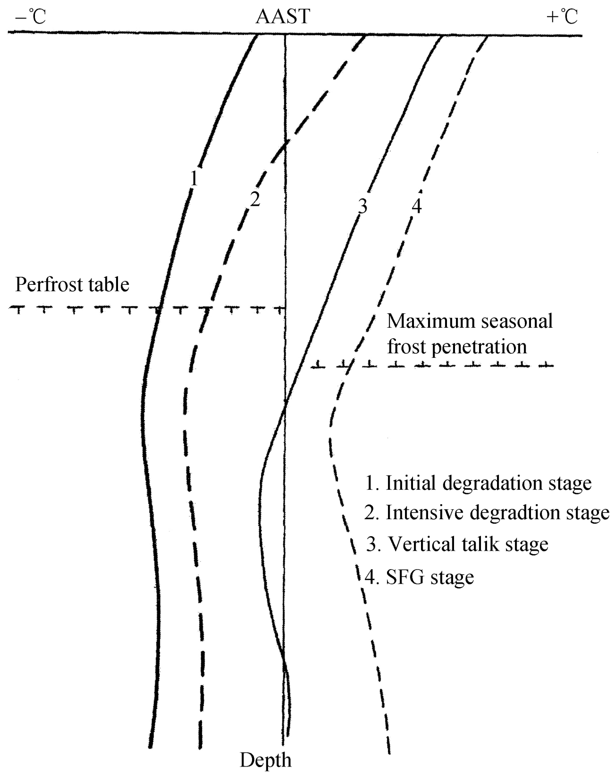

Fig. 4. Schematic diagram for downward permafrost degradation stages.

(i) Initial degradation. This stage of permafrost degradation can be illustrated by the results obtained from Boreholes K3363+800 and K3411+810 (Table 2). The AASTs at all depths are subzero and in the seasonally thawed layer decrease downwards, to depths below the permafrost table, when the geothermal gradients approximate zero or AASTs fluctuate in proximity to freezing/thawing temperatures of ambient soils. The AASTs were −1.04±0.01℃, i.e., with a thermal gradient of about zero at depths from 3 to 10 m in the Borehole K3363+800. The AASTs were −0.35±0.02℃, i.e., with a thermal gradient of about zero at depths from 5.15 to 10.65 m in Borehole K3411 + 810. These types of ground temperature curves indicate that permafrost has started to degrade downwards.

(ii) Intensive degradation. With the continued rising of air temperatures, the AASTs become positive at certain depths in the seasonally thawed layer in some areas. The AASTs in the seasonally thawed layer decline downwards and reach the freezing temperatures of soils. Then, thermal gradients approximate zero, and the soil temperatures fluctuate around the freezing points of ambient soils at certain depths below the permafrost table. This phenomenon was observed in Borehole K2936+400, with positive AASTs at depths shallower than 1 m. A similar situation also was observed in Borehole K2959+970, where the vertical section with positive AASTs was as thick as 1.5 m. In the borehole at the Sino-Japan Joint Observation Site (SJJOS) D66, AASTs were greater than 0℃ at depths above 4 cm, and those above 2.63 m in depths were warmer than −0.3℃. They all indicate that permafrost in these areas is degrading intensively.

(iii) Layered talik. With further rising of ground temperatures, when the depth with positive AASTs above the permafrost table surpasses the depth of seasonal frost penetration, permafrost is disconnected from seasonal frost, forming a thawed layer (layered talik). If the degradation process continues downwards, deeply buried permafrost remains. In Borehole K3393 + 950, the AASTs were positive at depths above 3.5 m, and permafrost was insulated from the seasonal frost. Similarly, AASTs were positive at depths above 2.45 m at the SJJOS Noda and a layered talik is starting to develop. Similar phenomena also were detected at the

Table 2　Statistics of annual average soil temperatures (℃) in shallow boreholes along the Qinghai-Tibet Highway

Type	Borehole	N. Lat.	E. Long.	Elev. (m)	Year	Thaw depth (m)	Depth (m) 0.04	0.10	0.20	0.40	0.50	0.60	0.80	1.00	1.15	1.30	1.50	1.60	1.65	1.80	2.00	2.15	2.30	2.34	2.42	2.45	2.50	2.63	2.65	2.71	2.80
Permafrost	K2936+400	35°31′43″	93°43′50″	4,557	1997—1999	2.1—2.2					0.16			0.09			–0.27				–0.68						–0.70				
	K2959+970	35°23′30″	93°31′40″	4,485	1997—1999	3.2—3.3					0.55			0.28			0.21				–0.12						–0.10				
	K3363+800	32°42′10″	91°52′35″	4,980	1998—1999	2.6—2.7					–0.77			–0.78			–0.95				–0.96						–0.98				
	K3393+950	32°29′33″	91°49′30″	4,850	1998—1998	3.5—3.6										0.64				0.59			0.35								0.21
	K3411+810	32°22′53″	91°42′54″	4,720	1998—1999	1.7—1.8									–0.07				–0.16			–0.21							–0.26		
	SJJOS D66	35°31′24″	93°47′50″	4,560	1998—1998	3.0—3.2	0.00		–0.10	–0.10		–0.10	-0.10	-0.20		–0.20		-0.20			–0.20							–0.30			
	SJJOS D110	32°41′29″	91°52′34″	4,977	1998—1998	2.2—2.3	0.50		0.20	0.30		0.10	-0.10	-0.30		–0.30		-0.40		-0.50											
	SJJOS Noda	32°27′36″	91°48′00″	4,850	1998—1998	2.6—2.7	1.10		0.80	0.90		0.80	0.70	0.60		0.50		0.50			0.20					0.10					
							Depth (m) 3.00	3.15	3.30	3.50	3.65	3.80	4.00	4.15	4.30	4.50	4.65	4.80	5.00	5.15	5.30	5.50	5.65	5.80	6.00	6.15	6.30	6.50	6.65	6.80	7.00
	K2936+400						–0.77			–0.86			–0.87			–0.86			–0.86			–0.87			–0.88			–0.88			–0.88
	K2959+970						–0.10			–0.29			-0.32			–0.53			-0.51			-0.50			-0.53			–0.60			–0.70
	K3363+800						–1.03			–1.03			-1.04			–1.03			-1.03			-1.03			-1.03			–1.03			–1.04
	K3393+950								0.02			–0.15			-0.21			-0.24			-0.25			-0.25			-0.26			–0.25	
	K3411+810							–0.29			-0.31			–0.33			–0.34			-0.36			-0.36			-0.36			–0.37		
							Depth (m) 7.15	7.30	7.50	7.65	7.80	8.00	8.15	8.30	8.50	8.65	8.80	9.00	9.15	9.30	9.50	9.65	9.80	10.00	10.15	10.30	10.65	10.80			
	K2936+400								–0.94			–0.98																			
	K2959+970								–0.72			–0.81																			
	K3363+800								–1.03			–1.04			–1.03			–1.04			–1.05			–1.04							
	K3393+950							–0.25			–0.25			–0.25			–0.24			–0.24			–0.23			–0.23		–0.22			
	K3411+810						–0.37			–0.37			–0.36			–0.36			–0.36			–0.36			–0.36		–0.35				
							Depth (m) 0.04	0.10	0.20	0.40	0.50	0.60	0.80	1.00	1.15	1.30	1.50	1.60	1.65	1.80	2.00	2.15	2.30	2.34	2.42	2.45	2.50	2.63	2.65	2.71	2.80
SFG	SJJOS Tuotuohe	34°13′01″	92°26′02″	4,533	1998—1998	3.5			1.60	1.60		1.30	1.40	1.20		1.20		1.10			1.30		1.40							1.50	
	SJJOS Amdo	32°14′28″	91°37′30″	4,710	1998—1998	3.5	1.30		1.30	1.60		1.30	1.30	1.30		1.40		1.30			1.30										1.20
	SJJOS MS3608	31°13′36″	91°47′01″	4,610	1998—1998	2.1	3.10		3.00	2.90		2.90	2.80	2.80		2.80		2.80			2.70				2.70						
	SJJOS MS3637	31°01′03″	91°39′26″	4,660	1998—1998	1.6		2.70	2.90	2.50		2.70	2.90	3.00		3.30		3.40			3.30			3.30							

southern and northern LLPs along the QTH[7,14].

(iv) Seasonally frozen ground (SFG). When the AASTs at all depths are significantly greater than 0 °C (generally about 1—3℃), permafrost thaws completely, and is replaced with SFG. The AASTs ranged from 1.1 to 1.6℃ at depths above 2.71 m at the SJJOS Tuotuohe Riverside. The drilling indicates that this location is now in the talik area. The SJJOS Amdo is now in the SFG area near the southern LLP. The maximum depth of seasonal frost penetration was 3.5 m. The AASTs varied from 1.2 to 1.6℃ at depths from 1 to 2.79 m. For another example, the AASTs at the depth of maximum frost penetration (2.1 m) was 2.7℃, and those at depths from 0 to 2.42 m ranged from 2.7 to 3.1℃ at the SJJOS MS 3608. The AAST at the maximum frost penetration (1.6 m) was 3.4℃ at the SJJOS MS 3637, and those at depths from 0 to 2.34 m ranged from 2.7 to 3.1℃. These observations indicate that permafrost in these areas has been completely transformed to SFG.

2.2 Upward degradation of permafrost

When the rates of heat loss in permafrost are less than the geothermal flows as a result of continual rising ground temperatures and subsequent diminishing geothermal gradients, permafrost degrades upward. Although local factors such as thermal conductivity, ice contents and ground water activities have great influences, the intensity and rates of upward permafrost degradation are determined by the ratio of the geothermal gradient in unfrozen soils below the bottom of permafrost and that in permafrost ($\boldsymbol{q}_{\mathrm{unf}}/\boldsymbol{q}_{\mathrm{p}}$). The greater the ratio, the more rapidly permafrost degrades upward.

Systematic analyses of geothermal data from 10 boreholes penetrating through permafrost thicker than the depths of zero annual amplitude of ground temperatures, and with observations over significantly long periods[18], indicate that the geothermal gradients of unfrozen soils ($\boldsymbol{q}_{\mathrm{unf}}$) below the base of permafrost were greater than those in permafrost ($\boldsymbol{q}_{\mathrm{p}}$) in 8 out of the 10 boreholes. The geothermal gradients in permafrost generally ranged from 0.04 to 0.07℃ m^{-1}, with a minimum of 0.02℃ m^{-1}. Those of unfrozen soils varied from 0.05 to 0.10℃ m^{-1}, with a minimum of 0.03℃ m^{-1}. Therefore, the ratios ($\boldsymbol{q}_{\mathrm{unf}}/\boldsymbol{q}_{\mathrm{p}}$) varied from 1.1 to 2.0. The average upward geothermal flow from underlying unfrozen soils was 83 mW m^{-2}, while the average upward geothermal flow from permafrost to ground surface was 64 mW m^{-2}, i.e., the permafrost layer received a net heat flow of 19 mW m^{-2}. Computations indicate that upward thawing rates in permafrost would range from 1.2—3.2 cm per year without considering climatic warming. However, under the combined influences of these geothermal flows and warming climate during the past several decades, the majority of ground temperatures have been rising and geothermal gradients in the warm permafrost layer have been approximating zero. When the unfrozen soils below permafrost are warmed, geothermal fluxes would further increase, subsequently enlarging the ratio of $\boldsymbol{q}_{\mathrm{unf}}/\boldsymbol{q}_{\mathrm{p}}$ and accelerating the upward degradation of permafrost.

The permafrost degradation in the Borehole at the Northern Outlet of Jingxian'gu Valley near the northern LLP is representative of upward permafrost degradation (Fig. 2(d)). Based on geothermal data in 1979, the bottom of permafrost then was at the depth of 14 m, and the MAGT +0.2℃. The geothermal gradient in the permafrost layer was 0.07℃ m^{-1}, while that in the unfrozen layer below permafrost was 0.08℃ m^{-1}. Thus, the ratio of $\boldsymbol{q}_{\mathrm{unf}}/\boldsymbol{q}_{\mathrm{p}}$ approximated 1.3 and permafrost had been degrading upwards at a rate of 2.7 cm per year, without considering climatic warming and lateral heat fluxes. The geothermal data from the same borehole in 1998 indicated that the bottom of permafrost had risen to 8 m in depth, and the MAGT had risen to +0.4℃. The geothermal gradient in the permafrost layer was 0.03℃ m^{-1} while that in the unfrozen layer below permafrost was 0.11℃ m^{-1}. Thus, the ratio of $\boldsymbol{q}_{\mathrm{unf}}/\boldsymbol{q}_{\mathrm{p}}$ approximated 3.7. The increased ratio resulted in accelerated thawing rates. During the past 20 years, 6 m of permafrost has been degraded in this borehole, with an average rate of upward degradation at 30 cm per year.

The borehole at the CAS Xidatan Observation Site also is located on a high flood plain 2 km away from the Borehole at the Northern Outlet of Jingxiangu Valley. The bottom of permafrost had been at 24.58 m in the CAS Xidatan Borehole drilled to a depth of 30.65 m in 1983; the MAGT observed at this borehole had been –0.4℃ in 1983. The bottom of permafrost rose to the depth of 20 m, and the MAGT was –0.1℃ based on measurements on 15 July 1998. During the period from 1983 to 1998, about 4.58 m (in thickness) of permafrost had thawed by upward degradation, with an average rate of degradation of 30 cm per year. Apparently, permafrost at these two boreholes has been degrading at similar rates.

Upward degradation of permafrost also was observed in Borehole 103-II-1 on a permafrost island in the Wenquan Valley (Fig. 3(d)). The borehole was drilled to a depth of 20 m on 5 August, 1976. The permafrost table then was at 3.5 m, the base of permafrost at the depth of 7.0 m, and the MAGT was +2.5℃. Based on the measurements on 13 August, 1998, the bottom of permafrost had already risen to the depth of 4.5 m. About 2.5 m (in thickness) of permafrost had degraded upwards from 1976 to 1998, with an average rate of permafrost degradation at 12.5 cm per year. Permafrost is now absent at this location.

In some areas, permafrost has been degrading both upwards and downwards. For example, the 31.4-m-deep Borehole Xidatan III-4 (Fig. 3(c)) was drilled on 23 June 1975. The bottom of permafrost was estimated at 20 m. However, on 25 May 1989, permafrost was found only from 8 to 11 m in depth, and AASTs from 13 to 30 m rose by 0.3 to 0.4℃[14]. The 2-directional thawing had accelerated permafrost degradation. At present, the site is free of permafrost.

2.3 Lateral degradation of permafrost

On the margins of permafrost islands, because of the higher temperatures of unfrozen soils and zero vertical thermal gradients, heat is more easily transferred laterally to permafrost. Therefore, lateral permafrost degradation is predominant in this case. In some areas, combined with upward and downward degradation, permafrost degradation can be greatly accelerated. Two examples well illustrate this phenomenon.

There was a permafrost island at Xidatan 150 m north of Milestone K2882 along the QTH. The island was about 150×100 m in size in the 1970s. Borehole No. 3 was drilled to a depth of 12 m on 15 June, 1975. The base of permafrost was at the depth of 11 m, and the thermal gradient was about 0 (Fig. 3(b)). However, permafrost was absent in Borehole No. 2, which is only 110 m away. On 25 May, 1989, the ground temperatures were positive at depths below 4 m in Borehole No. 3, and the thermal gradient was still almost zero. The drilling in June 1991 indicated that permafrost island had been converted to SFG.

Island permafrost is present in the Liangdaohe Basin, with a total area of about 4.74 km^2, in the southern section of the QTH. There are three types of frozen soils in this basin: 1) stable permafrost, 2) degrading permafrost, and 3) SFG (Fig. 5). The thicknesses of permafrost vary significantly from 0 on the margins of permafrost islands to 80 m near Borehole CK7 southwest of the QTH. The change is abrupt in the spatial distribution of permafrost, and permafrost is absent about 200 m away. By comparison of permafrost distribution maps compiled in 1975[12] (Fig. 5A) and 1996 (Fig. 5B), it is obvious that the areal extents of different types of frozen soils had changed during the 20 year period (Table 3). These two maps also reveal the complicated situations of permafrost degradation in the Laingdaohe Basin. Horizontally, stable permafrost (Area I) was partially transformed into degrading permafrost (Area II). Some degrading permafrost was changed to SFG (Area III). As a result, the areal extent of stable permafrost was reduced by 28.9%, whereas the areal extents of degrading permafrost and SFG were increased by 18.8 and 35.6%, respectively (Table 3). Although there are differences in the degradation modes of permafrost of varying thermal stability, lateral degradation has been playing a major role in the transformation from stable to degrading permafrost, or further to SFG. Ground temperature curves on a permafrost island in the Liangdaohe Basin on 16 April 1976 are shown in Fig. 3(e). Boreholes CK7 and CK2 were then in the center of the permafrost island, Borehole CK5 was on the edge, and Borehole CK4 was in the outside area of SFG (Fig. 5). From the ground temperature curves in the four boreholes, it is obvious that there were approximately zero vertical thermal gradients in all boreholes, and inward hori-

Table 3 Changes in areal extent (km^2) of various types of frozen ground in Liangdaohe Basin

Year	Total area	Area I	Area II	Area III
1975 (Map A)	4.74	2.49	0.48	1.77
1996 (Map B)		1.77	0.57	2.40
Area change (%)	100	–28.9	+18.8	+35.6

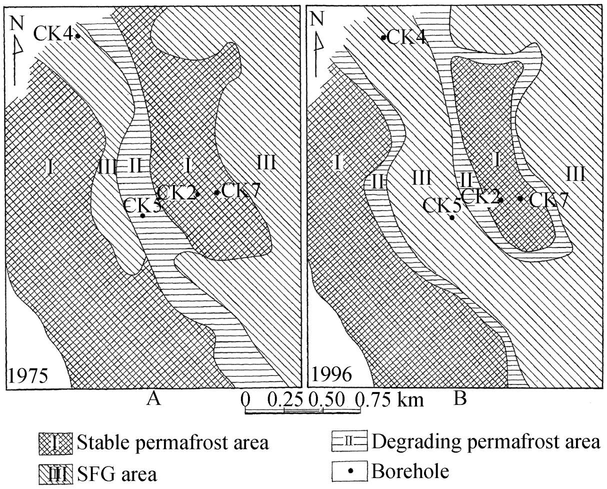

Fig. 5. Distribution of frozen ground at HMS 123 in the Liangdaohe Basin.

zontal geothermal gradients. The permafrost island has been shrinking due to the lateral degradation of permafrost. The Observation Sites (OS) No. 1 and No. 2 were respectively established in the center and on the edge of the permafrost island. The Boreholes CK2 and CK5 were in OS No. 1 and No. 2, respectively (Table 4). Heat fluxes at various depths in the two boreholes were measured daily from December 1975 to November 1976 using heat flux meters [19]. There was a conspicuous difference in heat fluxes between the two observation sites. The soils at OS No. 1 were receiving heat, while those at OS No. 2 were losing heat. At the permafrost table, the mean annual heat flux was +22 mW m^{-2} at the depth of 1.8 m at OS No. 1, while it was −22 mW m^{-2} at the depth of 3.2 m at OS No. 2. Although the heat fluxes were about the same, the directions were opposite. The data on heat fluxes agree with the AAST curves in Fig. 3(a), confirming the existence of lateral heat flows.

The analyses of heat fluxes at the bottom of the permafrost at 59.8 m in Borehole CK7 indicate that ground temperatures change linearly with depths below 45 m (Fig. 3(e)), confirming a stable upward geothermal flow. The mean annual heat flux was −11 mWm^{-2} at 59 m (Table 4). If the geothermal gradient below the depth of 45 m is taken as 0.01℃ m^{-1}, there was an upward heat flow of about 31 mW m^{-2} at the bottom of the permafrost island. This value is slightly smaller than the range (36—142 mW m^{-2}) of heat

Table 4 Heat fluxes (mW m^{-2}) at the Liangdaohe Observation Sites (revised from ref. [19])

	Heat flow (mW m^{-2})	1975	1976											Annual average
		Dec	Jan	Feb	Mar	Apr	May	Jun	Jul	Aug	Sep	Oct	Nov	
Observation Site No. 1	Depth (m) 0.07	−11.39	−8.83	−2.43	−2.47	−1.33	8.48	8.45	7.09	5.76	2.87	−1.02	−7.72	−0.21
	0.20	−10.32	−5.97	−2.25	−0.80	0.67	5.69	9.61	7.85	6.66	2.71	0.09	−3.02	0.91
	0.40	−7.48	−4.73	−1.91	−0.39	0.66	1.23	2.21	6.41	5.53	3.07	0.23	−0.02	0.40
	0.67	−6.73	−7.70	−3.67	−1.20	0.37	1.30	0.91	2.68	5.10	3.37	0.37	0.00	−0.43
	1.20	−0.21	−4.19	−2.91	−0.95	0.06	0.65	0.88	0.81	1.28	3.56	0.65	0.07	−0.02
	1.80	0.15	0.04	−2.34	−1.06	−0.09	0.35	0.48	0.57	0.56	0.65	0.49	0.48	0.02
	2.10	0.18	0.35	−1.75	−1.04	13.93	0.29	0.42	0.48	0.49	0.59	0.45	0.45	1.24
	2.40	0.28	0.27	−0.70	−0.88	−0.22	0.21	0.28	0.39	0.38	0.44	0.37	0.42	0.10
	2.80	0.23	0.26	0.23	−0.96	−0.29	−0.12	0.18	0.28	0.31	0.31	0.26	0.28	0.08
	3.20	0.18	0.18	0.14	−0.46	−0.19	0.07	0.07	0.26	0.33	0.28	0.19	0.20	0.10
	8.00	0.00	−0.02	−0.01	0.00	0.04			0.02	0.04	−0.02	0.00	−0.01	0.00
	13.00	0.00	0.00	0.00	−0.02	0.00			−0.01	−0.02	−0.04	−0.01	−0.01	−0.01
	18.70	0.01	0.00	0.01	0.00	0.01			0.01	0.02	0.00	0.02	0.02	0.01
	40.00	0.01	0.01	0.01	0.01	0.01			0.00	0.00	−0.01	0.00	0.00	0.00
	59.00	0.01	0.01	0.02	0.01	0.01			−0.02	−0.05	−0.06	−0.02	−0.02	−0.01
Observation Site No. 2	0.13	−13.35	−8.59	−5.93	−2.07	3.43	7.03	4.69	4.73	2.81	−1.56	−4.21	−6.85	−1.66
	0.40	−6.56	−4.84	−1.94	−0.59	0.53	5.17	4.41	3.76	1.81	0.66	−1.30	−3.25	−0.18
	0.80	−6.44	−5.01	−2.45	−1.04	0.08	3.31	4.59	3.46	2.53	1.34	−0.89	−1.67	−0.18
	1.38	−4.08	−3.93	−2.59	−1.22	−0.33	0.42	2.51	2.88	2.32	1.43	−0.12	−0.42	−0.26
	1.60	−2.46	−3.14	−2.18	−1.04	−0.37	0.46	1.73	2.66	2.16	1.54	0.00	−0.36	−0.08
	3.20	−0.18	−0.14	−1.01	−1.10	−0.60	0.07	−0.09	0.02	1.35	1.45	0.51	0.04	0.03
	19.50	−0.01	0.02	0.00	0.00	−0.02	0.00	0.02	0.01	0.02	0.05	−0.04	−0.02	0.00

flows at the bottom of permafrost along the QTH[18]. Therefore, while the lateral degradation is obvious, upward and downward degradation of permafrost also have been working. The ground temperature at the depth of 59.8 m has risen by 0.1℃, confirming the upward degradation. The lateral degradation of permafrost has been causing the areal shrinkage and has caused the rise of ground temperatures in the stable permafrost (Area I). For example, a general rise of 0.1 to 0.2℃ in ground temperatures at depths from 15 to 59.8 m in Borehole CK7 in the center of the permafrost island was observed from the 1970s to 1990s. Permafrost on the edges had been transformed to SFG (Fig. 5). Borehole CK5 drilled to a depth of 19.5 m on 17 June, 1975 was originally located inside the OS No. 2 in the stable permafrost area. The MAGT was about 0℃ and there was a section of zero geothermal gradients above 8 m in depth on 15 September, 1975. At the base of permafrost at 19.5 m, the average annual heat flow was +11 mW m^{-2}, indicating heat-absorbing permafrost. Ground temperature measurements on 6 August, 1984 indicate the absence of permafrost, which might have been caused by lateral thawing. The lateral degradation enlarged the area of degrading permafrost (Area II) by reducing the area of stable permafrost (Area I), and increased the area of SFG (Area III) by the reduction in area of degrading permafrost (Area II). The rising of ground temperatures is a general trend in the Liangdaohe Basin[7]. At present, permafrost around Borehole 123-5 has been completely changed to SFG (Fig. 5B). The SFG area (Area III) increased by 35.6% from 1975 to 1996 (Table 3). The ground temperatures also had risen by about 0.2 to 0.3℃ at depths from 15 to 19.5 m in Borehole CK4 from 1975 to 1983.

The modes of permafrost degradation in the Liangdaohe Basin fully illustrate the characteristics of permafrost degradation along the QTH. The ground temperatures of thicker, stable permafrost have been rising. On the margins of stable permafrost areas, permafrost has been degrading remarkably. The original degrading permafrost has been converted to SFG. Horizontally, permafrost has been retreating toward the center of permafrost islands. Vertically, upward and downward degradation of permafrost of different types at various depths has occurred simultaneously with lateral degradation, forming the present distribution of permafrost.

3 Summaries and discussions

Based on the observations and analyses of ground temperatures and the degradation modes of permafrost along the QTH, it is summarized that:

1) In recent years, permafrost along the QTH has been degrading and retreating regionally under a warming climate. Based on the features of ground temperature curves, permafrost has been divided into three types: stable, degrading, and phase-changing transitory permafrost.

2) Spatially, permafrost can degrade downwards, upwards and laterally. The ultimate results are thinning and/or the complete disappearance of permafrost. However, there are strong differentiations in localities and at depths.

3) When seasonal thaw penetration exceeds seasonal frost penetration, downward degradation of permafrost starts. Under the influence of warming surface temperatures, the geothermal gradients in permafrost keep dropping. Upward or lateral degradation begins when geothermal gradients in permafrost are smaller than in the underlying or ambient unfrozen soils.

4) In the type of downward degradation of permafrost, four stages can be subdivided based on the characteristics of changes in ground temperatures near the permafrost table. They are: initial degradation, intensive degradation, layered talik, and disappearance of permafrost to SFG. These four stages illustrate the entire degradation process from permafrost to SFG.

5) Recent climatic warming has led to regional retreat and degradation of permafrost as evidenced by the reduction of permafrost area and the rising of ground temperatures to as deep as 60 m. It is projected that the trend of permafrost degradation will persist and affect permafrost in wider areas and to deeper depths during the 21st century.

6) The major factors controlling the thickness of elevational permafrost and its changes include ground surface temperature and its evolutional history, topography, geothermal flow and its variability, and the vertical zonation of permafrost[20,21]. Permafrost has been

retreating poleward and to higher elevations in the northern hemisphere due the climatic warming since the Holocene. The retreating has been accelerating since the end of the Little Ice Age. For example, the upward thawing rate of warm permafrost in the discontinuous permafrost zone in Alaska reportedly has been about 4 cm per year under a warming of 0.5 to 1.5℃ during the past 20 years[22,23]. This number is much smaller than that (12 to 30 cm per year) along the QTH. One of the major reasons for better protection of permafrost and thus slower degradation in south-central Alaska is due to the larger thermal offsets of generally thick organic and moss surface layers. However, in the sporadic permafrost zone, lateral degradation is active, which works together with downward degradation, resulting in widespread thermokarsts in ice-rich permafrost areas[15,16]. In comparison, downward thawing rates of ice-rich permafrost in central Mongolia are 3 to 7 cm per year under a warming of 0.15 to 0.45℃ during the past 30 years[24]. It is predicted that permafrost thinner than 25 m would disappear and an upward thawing of 1.0 to 2.5 m of permafrost would occur in areas with permafrost thickness greater than 50 m by the middle 21st century. Although island and sporadic permafrost would be lost, continuous and discontinuous permafrost would not decline as remarkably (<20%—25%). Downward and upward thawing of deeply buried permafrost in central part of western Siberia[25] also supports the observed 3-directional global degradation of warm permafrost. However, there are reports that the thermal state of the upper 15 m of permafrost in central Yakutia, Siberian Russia has remained stable under a warming climate, which is attributed to the modes of rising air temperatures and decreasing snowfall[26]. Under a warming continental climate, abrupt interannual or substantial warming enormously impacts the degradation of permafrost[27]. For example, an occasional or consecutive hot summer(s) with average summer temperatures 5 to 6℃ warmer than normal would greatly enhance the deepening of seasonal thaw penetration and development of layered talik at timescales of 10 to 20 years[1)]. Sudden changes in micro-topography and surface coverage, such as the removal of vegetation and organic layers necessitated by engineering construction, or by flooding, greatly influence the thermal stability of permafrost. For example, a warmer winter with less snowfall may tend to cool the soils more than a cold winter with more snowfall in central Yakutia[26]. Therefore, the uncertainties in degradation processes of permafrost remain large.

The present rates of downward and upward degradation of permafrost along the QTH were 6—25 and 12—30 cm per year, respectively. Compared to the values in the arctic, permafrost along the QTH degrades much more rapidly, which is attributed to the higher initial ground temperatures, geothermal flows by active tectonics, thin permafrost, and substantial and persistent climatic warming. However, in the sections with strong influences from abnormally high geothermal flows, ground and surface waters, and engineering activities, the rates of permafrost degradation are remarkably larger. For example, lateral degradation of permafrost ranges from 62 to 94 cm per year in Xidatan in the island permafrost zone. However, the upward thawing of thicker permafrost would be smaller because the effects of surface and atmospheric climatic warming are relatively minor at depths. It is projected that island permafrost would disappear, the taliks in the interior of the QTP would expand significantly, and the predominant MAGTs would shift from the present –1.5—–0.5℃ to –0.4—0℃, with a total reduction of permafrost area of about 18% by the middle of the Twenty-first century, assuming a warming of 1.1℃[28]. Another prediction indicates that permafrost in the eastern, northern, and southern QTP would largely disappear, and its total area would shrink by 58% by 2100, assuming a 2.91℃ increase in air temperature[29]. However, many assumptions and simplifications compromise the accuracies of models because the stochastical processes of climatic change in reality differ significantly from the climatic change scenarios assumed in prediction models. There also is a great unevenness in the distribution of data on the plateau and the spatial parameterization of data needed

1) Jin H, Brewer M C. Highway roadway stability influenced by warm permafrost and seasonal frost action. J Cold Reg Eng, 2006, accepted

in models becomes quite challenging. As a result, these models and their outputs still require more substantial research by observations and spatio-temporal down- or up-scaling of permafrost models. Paleo-reconstruction using relic permafrost phenomena and ground temperatures is still rudimentary along the QTH and on the QTP, compared with other paleo-reconstruction using ice cores, tree rings and lacustrine sediments. Further research is needed on the degradation modes, and processes of permafrost since the hypsithermal and postglacial periods.

In summary, the major inadequacies of research on the modes of permafrost degradation include inadequate and uneven spatial distribution of data, too short and frequently interrupted data series, insufficient observations from boreholes that cut through permafrost, information on geothermal fluxes, inadequate in-depth simulation and modeling, and lack of resolution of disputes on the relationships between the evolution of permafrost, glaciers, and lakes. More urgent issues on the modes of permafrost degradation would include observations, modeling and forecasting of permafrost degradation under influences of sudden, gradual or oscillating climatic change, and engineering activities. It is only possible to correctly or more objectively evaluate the ecological, environmental, hydrological and engineering impacts of permafrost degradation, and make policies that look for engineering and managerial solutions for these impacts when the degradation modes and processes of permafrost are understood.

Acknowledgements The authors are grateful to Prof. Max C. Brewer, former Arctic Engineer and Geologist with U. S. Geological Survey Alaska Science Center, carefully reviewed and edited the English contents and provided many insightful revisions. The authors also would like to acknowledge the additional assistance from Lü Lanzhi and He Baoshan with Laboratory Technicians at CAREERI, CAS for drawing some of the figures. This work was supported by CAS Hundred Talents Program "Stability of linear engineering foundations in warm permafrost regions under a changing climate" (2004), and CAS Knowledge Innovation Key Programs (Grant Nos. KZCX1-SW-04, KZCX3-SW-345 and KZCX3-SW-339-3).

References

1 Wang S L. Discussions on the formation and evolution of permafrost on the Qinghai-Tibet Plateau since the Late Pleistocene. J Glaciol Geocryol (in Chinese), 1989, 11(1): 67—75
2 Zhou Y W, Guo D X, Qiu G Q, et al. Permafrost in China (in Chinese). Beijing: Science Press, 2000. 377—386
3 Qiu G Q, Cheng G D. Permafrost in China: past and present. Pf & Periglac Proc, 1995, 6(1): 3—14
4 Cheng G D, Wang S L. Discussions on the zonation of altitudinal permafrost in China. J Glaciol Geocryol (in Chinese), 1982, 4(2): 1—17
5 Jin H J, Li S X, Wang S L, et al. Impacts of climatic changes on permafrost and cold regions environments in China. Acta Geogr Sin (in Chinese), 2000, 55(2): 161—173
6 Cheng G D. Some difference of permafrost on the Qinghai-Tibet Plateau of China and northern Canada. J Glaciol Geocryol (in Chinese), 1980, 2 (1): 39—42
7 Wang S L. Changes of permafrost along the Qinghai-Tibet highway during the past several decades. Arid Land Geogr (in Chinese), 1993, 16(1): 1—8
8 Jin H J, Cheng G D, Li X, et al. Permafrost on the Qinghai-Tibet Plateau under a changing climate. Chin Sci Bull, 1999, 44(Supplement): 152—158
9 Nan Z T, Li S X, Wu T H. Changes of permafrost at Xidatan on the Qinghai-Tibet Plateau during the past 30 years. Acta Geogr Sin (in Chinese), 2003, 58(6): 817—823
10 Dou M J. Discussion on permafrost stability along the Qinghai-Tibet Highway. J Glaciol Geocryol (in Chinese), 2000, 22(Supplement): 92—97
11 Wu Q B, Zhu Y L, Liu Y Z. Evaluating models of frozen soil environment change under engineering actions. Sci China Ser D-Earth Sci, 2002, 45(10): 893—902
12 Wang S L, Zhao X F. Environmental changes in island permafrost areas along the southern section of the Qinghai-Tibet Highway. J Glaciol Geocryol (in Chinese), 1998, 20(4): 231—239
13 Wang G X, Sheng Y P, Cheng G D. Changes of ecological environments in the sources of the Yellow River and analyses on their causes. J Glaciol Geocryol (in Chinese), 2002, 22(3): 200—205
14 Wang S L, Jin H J, Li S X, et al. Permafrost degradation on the Qinghai-Tibet Plateau and its environmental impacts. Pf & Periglac Proc, 2000, 11(1): 43—53
15 Jorgenson M T, Racine C H, Walters J C, et al. Permafrost degradation and ecological changes associated with a warming climate in central Alaska. Clim Chang, 2001, 48: 551—579
16 Osterkamp T E, Jorgenson M T. Response of boreal ecosystems to varying modes of permafrost degradation in Alaska. Can J Forest Res, 2005, 35(9): 2100—2112
17 Wu Z W. Principal types of permafrost temperatures of the Qinghai-Tibet Plateau and computation methods of thermal parameters for engineering applications. In: CAS Lanzhou Institute of Glaciology and Geocryology, ed. Monograph on the Research of Permafrost on the Qinghai-Tibet Plateau (in Chinese). Beijing: Science Press, 1983. 185—194
18 Wang J C, Li S D. Analyses on the thermal regimes at the permafrost table along the Qinghai-Tibet Highway. In: CAS Lanzhou

Institute of Glaciology and Geocryology, ed. Monograph on the Research of Permafrost on the QTP (in Chinese). Beijing: Science Press, 1983. 38－43
19 Xu X Z, Zhu L N. Thermal and moisture regimes of islands permafrost at Liangdaohe in Tibet. In: CAS Lanzhou Institute of Glaciology and Geocryology, ed. Monograph on the Research of Permafrost on the QTP (in Chinese). Beijing: Science Press, 1983. 44－48
20 Nelson F E, Lachenbruch A H, Woo M K, et al. Permafrost and changing climate. In: Cheng G D, Qiu G Q, eds. Proceedings of the 6th International Conference on Permafrost, 5－9 July 1993, Beijing, China. Guangzhou: South China University of Technology Press, 2003. 987－1005
21 Sergueev D, Tipenko G, Romanovsky V, et al. Mountain permafrost thickness evolution under influence of long-term climate fluctuations (results of numerical simulation). In: Phillips M, Springman S M, Arenson L U, eds. Proceedings of the 8th International Conference on Permafrost, 21－25 July 2003, Zurich, Switzerland. Lisse: A. A. Balkema Publishers, 2003. 1017－1021
22 Osterkamp T E. A thermal history of permafrost in Alaska. In: Phillips M, Springman S M, Arenson L, eds. Proceedings of the 8th International Conference on Permafrost, 21－25 July 2003, Zurich, Switzerland. Lisse: A. A. Balkema Publishers, 2003. 863－868
23 Osterkamp T E, Gosink J P. Variations in permafrost thickness in response to changes in paleoclimate. J Geophys Res, 1991, 96(B3): 4423－4434
24 Sharkhuu N. Recent changes in the permafrost of Mongolia. In: Phillips M, Springman S M, Arenson L U, eds. Proceedings of the 8th International Conference on Permafrost, 21－25 July 2003, Zurich, Switzerland. Lisse: A. A. Balkema Publishers, 2003. 1029－1034
25 Ananjeva G V, Melnikov E S, Ponormareva O E. Relict permafrost in the central part of western Siberia. In: Phillips M, Springman S M, Arenson L U, eds. Proceedings of the 8th International Conference on Permafrost, 21－25 July 2003, Zurich, Switzerland. Lisse: A. A. Balkema Publishers, 2003. 5－8
26 Skcryabin P, Skachkov Y, Varlamov S. The thermal state of soils under contemporary climate change in Central Yakutia. In: Phillips M, Springman S M, Arenson L U, eds. Proceedings of the 8th International Conference on Permafrost, 21－25 July 2003, Zurich, Switzerland. Lisse: A. A. Balkema Publishers, 2003. 1063－1066
27 Riseborough D W, Smith M W. Modeling permafrost response to climatic change and climate variability. In: Lunadini V J, ed. Proceedings of the 4th International Symposium on Thermal Engineering and Science for Cold Regions, US Army CRREL Special Report 93－22, Hanover, NH, USA: US Army CRREL, 1993. 179－187
28 Li S X, Cheng G D, Guo D X. Numerical modeling of the trends of changes of permafrost on the Qinghai-Tibet Plateau under a persistently warming climate. Sci China Ser D-Earth Sci (in Chinese), 1993, 23(4): 342－347
29 Li X, Cheng G D. Model for studying the response of altitudinal permafrost to global change. Sci China Ser D-Earth Sci (in Chinese), 1999, 29(2): 185－192